An Experimental Study of Near-Field Cassegrainian Antennas*

By D. C. HOGG and R. A. SEMPLAK

(Manuscript received May 30, 1964)

The near-field Cassegrainian antenna is a double-reflector system that employs, in its simplest form, confocal paraboloids. Unlike the standard Cassegrain which employs a hyperboloidal subreflector illuminated by a spherical wave, the near-field device is fed by a uniform phase front. Experimental data on noise performance, gain, and radiation patterns have been obtained at a frequency of 6 gc using two 16-foot paraboloids (focal length-to-diameter ratios of 0.375 and 0.25) in both standard and near-field configurations.

Using the shallow antenna, zenith noise temperatures of 10°K and 6°K were obtained for the standard and near-field systems, respectively; at an elevation angle of 10° the antenna temperatures were 50°K and 20°K. Using the deep secondary reflector, zenith noise temperatures of 4°K were obtained for both configurations; at 10° above the horizon, however, the standard Cassegrain has an antenna temperature of 30°K and the near-field device 13°K. In all cases, the antenna efficiencies are not far above 50 per cent. Discussion of noise produced by various methods of mounting subreflectors is included. Since noise produced by transmission lines and antenna environment is closely related to these experiments, it is discussed in detail in appendices.

I. INTRODUCTION

Large microwave antennas of high efficiency and low noise are desirable in radio astronomy, in tracking of space probes and in satellite communications. In all of these cases, convenient access to the associated electronic equipment is also a desirable feature. The horn reflector[1,2] is an antenna which provides this access and also admirably satisfies the electrical requirements. Nevertheless, it is of interest to

* Part of this material was presented to the URSI in Washington, D. C. (May, 1962).

examine other types of microwave antennas of more favorable ratio of geometrical aperture to total size with a view to improvement of their electrical performance toward that of the horn reflector.

The purpose of this study is twofold: to evaluate the near-field Cassegrain as a microwave antenna, and to compare its noise performance with that of other antennas. Actually, two 16-foot diameter paraboloids have been tested, one with an f/D ratio of 0.375 and the other of 0.25. Measurements of antenna noise temperature, gain, and radiation patterns were made at a frequency of 6 gc using various feeding arrangements on both of these main reflectors.

Most paraboloids have relatively low aperture efficiencies and exhibit poor noise performance. For example, paraboloids fed by a horn at the focal point typically have intrinsic (back lobe) noise temperatures of 20 or 30 degrees Kelvin,[3,4] whereas the equivalent noise for the horn reflector is about 2°K.[5,6,7] This noise is due to thermal radiation from the environment of the antenna (mainly the ground) into the wide-angle or back lobes of the antenna; in what follows, it is designated by T_b.

Paraboloids fed by a source at the focus suffer from another deficiency: either the first circuit of the receiver must be mounted at the focal point (which is inconvenient), or a rather long transmission line (which results in a prohibitive increase in noise) must be provided. This undesirable feature is overcome by use of the Cassegrainian configuration[8,9] which, in the usual arrangement, has a point source feed at the apex of the main (secondary) reflector and a hyperboloidal (primary) subreflector near the focal plane. In this case, the receiving equipment may be situated at the apex of the secondary reflector, free space serving as the transmission medium to the subreflector. Often the location of equipment near the apex is restrictive; depending on the arrangement, it may or may not move with the main reflector. This type of feed is referred to here as the "standard" Cassegrain.

The near-field Cassegrain combines some of the useful properties of the horn reflector with those of the standard Cassegrain. Rather than a point-source feed at the apex of the main reflector, a plane-wave feed of the same dimension as the subreflector is used.* Of course, the subreflector blocks the field of the main aperture just as in the case of the standard Cassegrain configuration. The plane-wave feed used for the measurements to be discussed was a small horn-reflector antenna. This arrangement allows the electronic equipment to remain stationary while

* Experiments on an antenna of this type were described recently by Profera et al.[10] Some generalized antenna systems based on this concept are discussed by S. P. Morgan.[11]

the elevation angle of the antenna is changed, in much the same manner as with the horn-reflector antenna.

It should be mentioned that the near-field feeding system is suited only to antennas that are very large compared to the wavelength. In the model that has been tested here, where the antenna diameter is less than 100λ, this criterion is just met. However, it appears that the feed system is broadband, embracing all wavelengths shorter than that satisfying the criterion, and in this sense the near-field antenna is somewhat similar to the horn reflector. Methods for mode scanning[12] a horn-reflector antenna are equally applicable to a near-field Cassegrain.

In Section II, the geometry of the near-field Cassegrainian antenna is discussed; the fields produced by the near-field feed are also given there. Section III describes the equipment, siting, and the methods used for measurement of antenna noise temperature and gain. Sections IV and V contain the noise and gain measurements on the shallow and deep sixteen-foot paraboloids using various types of feeds; the effect of subreflector mounting structures on noise performance is also given in those sections. Measurement of noise due to loss in transmission lines is dealt with in Appendix A. In Appendix B, the back-lobe noise temperature (T_b) for an antenna in a given environment is discussed, and in Appendix C, a quality factor which governs the signal-to-noise ratio in antennas is proposed.

II. THE NEAR-FIELD CASSEGRAINIAN ANTENNA

2.1 *Comparison of Standard and Near-Field Cassegrainian Antennas*

The standard and near-field Cassegrainian antennas are compared in the idealized sketches of Fig. 1. An extensive analysis of the standard Cassegrain antenna has been given[8] and it will not be discussed further here; however, it should be noted that radiation from the point-source feed tends to spill over the rim of the hyperboloid. It has been demonstrated recently[13] that suitable beam shaping of the source pattern can reduce this spill-over. The receiving equipment is stationary as the antenna changes elevation, a right-angle circular waveguide bend and rotating joint being provided in the transmission line (see Fig. 1a). A simple right-angle bend would not be used in systems employing circular polarization since, due to unequal phase velocities of orthogonal components, the circularity would be degraded. A simple bend was used in the measurements to be discussed since circular polarization was not involved.

The near-field Cassegrain, shown in Fig. 1(b), has a horn-reflector

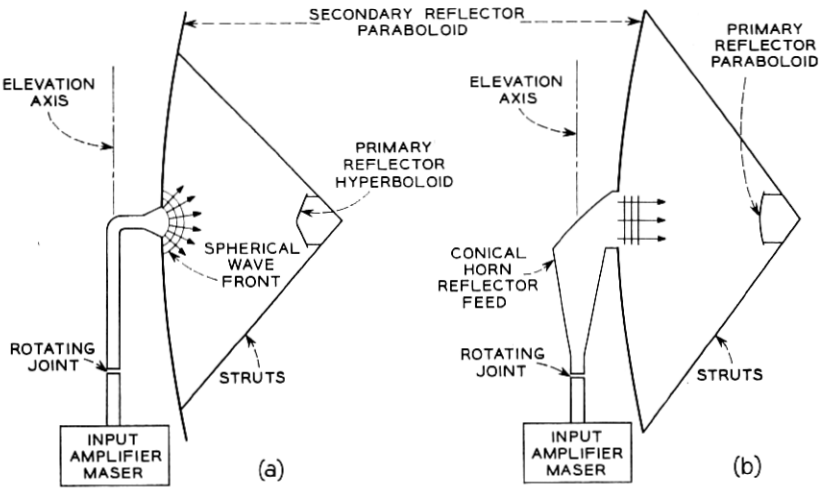

Fig. 1 — Idealized standard and near-field Cassegrainian antennas.

feed with an aperture of about the same diameter as that of the subreflector. To a geometrical optics approximation, the near field of this feed is collimated and of uniform phase.

2.2 *Geometry of Near-Field Cassegrain*

A simple derivation shows that the surface of the subreflector in the near-field configuration should be paraboloidal. Assume that the surface of the subreflector (see Fig. 2) is paraboloidal; it will then be sufficient to show that the path length of any ray from the plane wave in the feed aperture EF to a reference plane in the secondary aperture is constant. Consider the ray of path length $\overline{AB} + \overline{BC} + \overline{CD}$. Equating this path to the length of the axial ray, one has

$$\overline{AB} + \overline{BC} + \overline{CD} = 2(f - f_1) + f = 3f - 2f_1 \tag{1}$$

where f_1 and f are the focal lengths of the primary and secondary reflectors.* From Fig. 2, the line segments $\overline{AB}$, $\overline{BC}$, and $\overline{CD}$ are equal to $f - z_0$, $r_2 - r_1$, and $r_2 \cos\theta$ respectively. Equation (1) then becomes

$$f - z_0 + r_2 - r_1 + r_2 \cos\theta = 3f - 2f_1 \tag{2}$$

* Primary and secondary are used to designate the sub- and main reflectors respectively because the radiation patterns of the feed and main reflector are usually referred to as primary and secondary patterns.

where $z_0 = r_1 \cos \theta$, and from the equations of the paraboloids

$$r_1 = \frac{2f_1}{1 + \cos \theta} \quad \text{and} \quad r_2 = \frac{2f}{1 + \cos \theta}.$$

Making these substitutions, (2) becomes

$$f - \frac{2f_1(1 + \cos \theta)}{1 + \cos \theta} + \frac{2f(1 + \cos \theta)}{1 + \cos \theta} = 3f - 2f_1$$

which proves the equality.

As in the case of the standard Cassegrain, the degree of illumination on the surface of the secondary reflector of a near-field Cassegrain can be varied by using subreflectors of various focal lengths. Optimum illumination, as determined by geometrical optics, is achieved by using a subreflector of f/D ratio identical to that of the secondary reflector.

Fig. 3 is an idealized sketch of the near field along the axis of the source aperture, the relative positions of subreflectors used in the experiments being indicated by arrows. Note that the subreflectors are

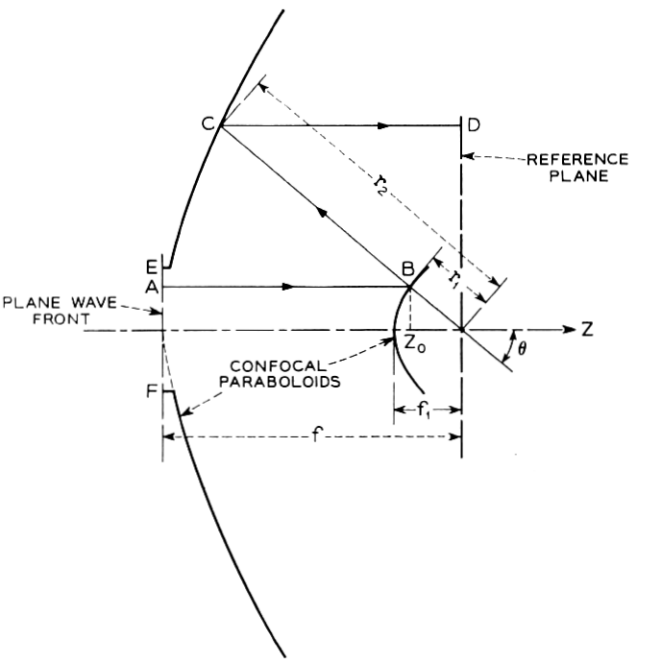

Fig. 2 — Geometry of near-field Cassegrainian antenna.

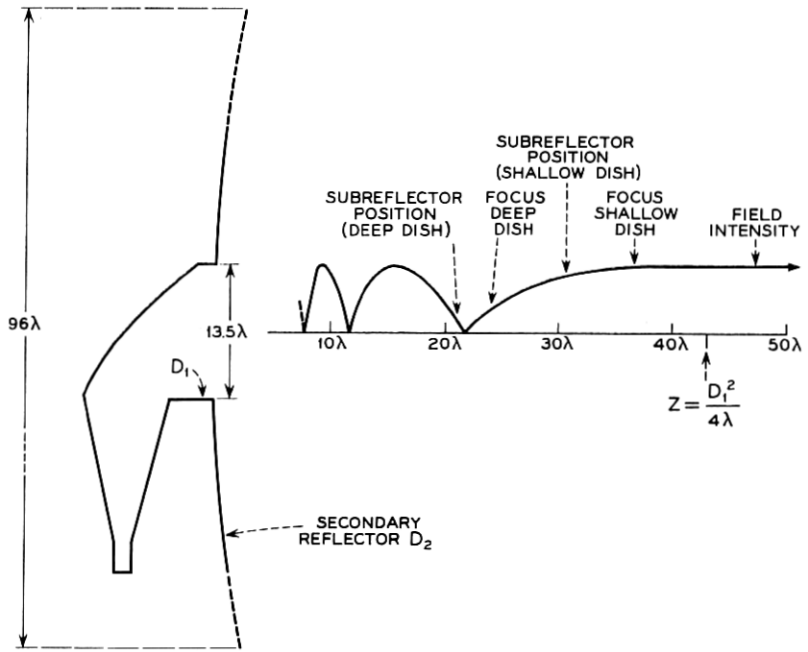

Fig. 3 — Idealized near-field along the axis of the feed.

well out in the near-field. As mentioned in the introduction, the antenna size and wavelength used for these tests are far from optimum for the near-field type of feed. Preferably one would choose dimensions as large as possible with respect to wavelength (a high-gain antenna) in which case geometrical optics would hold more rigorously; an immediate consequence of this is that the subreflector positions (see Fig. 3) would be located where collimation and phase uniformity of the near-field are greatly improved.

2.3 *The Conical Horn-Reflector Feed*

A horn-reflector antenna[14] was used as the near-field feed for both the shallow and deep dishes. Theoretical and experimental studies of the far-field characteristics of this antenna have been published;[2] here, discussion is confined to its near-field characteristics.

The first 16-foot diameter secondary reflector used in the near-field Cassegrainian configuration had a focal length of 6 feet; therefore measurements of amplitude and phase of the field were made six feet

in front of the aperture of the horn reflector, where the subreflector was to be mounted. The measurements were made in an anechoic chamber using a dipole probe. The data are plotted in Fig. 4 along with theoretical curves; these compare favorably in their general trend but not in detail. One notes that the phase departs from uniformity by about $\pm 10°$ in some cases and that it is unsymmetrical with respect to the axis.

III. EQUIPMENT AND METHODS OF MEASUREMENT

3.1 *Equipment*

Fig. 5 shows a complete antenna mounted on a motorized turntable carriage for azimuthal rotation. The cab to the left of the antenna is shielded; it houses the necessary equipment for measuring noise temperature, gain, and radiation patterns. The double A frame and cradle structure on which the secondary reflector is mounted is shown more clearly in Fig. 9 (p. 2691); it is a strong structural unit, no demand being made of the paraboloid for supplying rigidity. Elevation steering is provided by rotation of the cradle on bearings in the A frames. The transmission line, a circular waveguide of 2.8-inch diameter, is fed to the receiver in the cab through the bearing via a rotating joint.

The antenna is sited in a relatively flat, clear area; however, the site is ringed with trees which limit the horizon to an average elevation angle of 1.5 degrees.

The 6-gc maser receiver used for antenna noise temperature measurements has been discussed previously.[5,7]

3.2 *Method of Noise Measurements*

The setup used for measuring noise performance is shown in Fig. 6. The noise temperature at the input to the converter with the noise lamp off is given by

$$T_{ic} = G_m(T_a + T_m) \tag{3}$$

where G_m, T_m are the maser gain and noise temperature, and $T_a = T_s + T_l + T_b$ is the antenna temperature. T_s is the sky temperature observed by the main beam. T_l is the noise temperature of the transmission line associated with the antenna.* T_b is the noise contribution from the earth and sky through the wide angle side and back lobes of

* Here we neglect the actual attenuation due to transmission line loss; it is quite small.

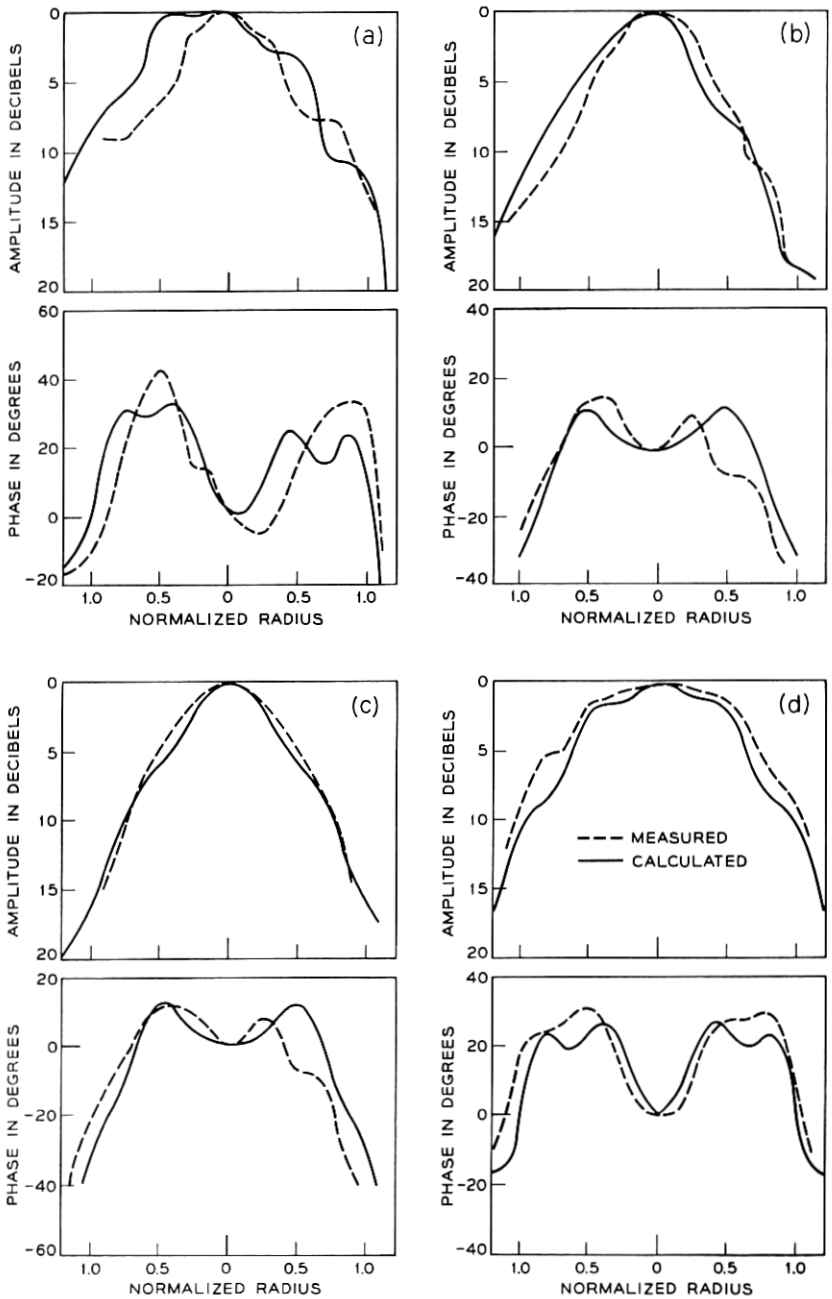

Fig. 4 — Near-field patterns of horn reflector (Z = 6 ft.).

Fig. 5 — A 16-foot diameter paraboloid (f/D = 0.375) with near-field Cassegrainian feed.

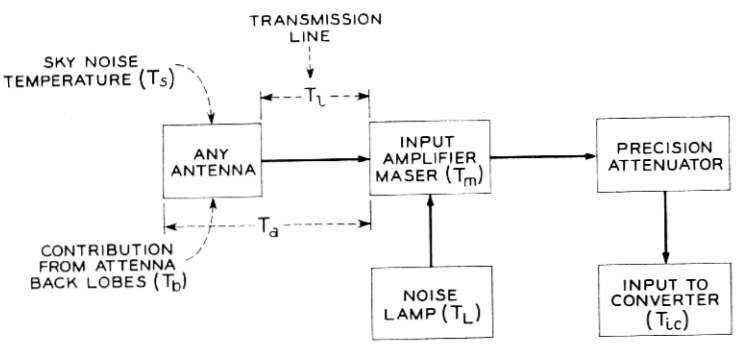

Fig. 6 — Noise contributors in the receiving system.

the radiation pattern. With the noise lamp fired, the noise input to the converter becomes

$$T_{ic} = G_m A(T_a + T_m + T_L) + (1 - A)T_0 \tag{4}$$

where T_L is the additional noise introduced by the calibrated noise lamp, T_0 the ambient temperature and A the reciprocal of the additional loss introduced by a precision attenuator to equalize (3) and (4).

Solving (3) and (4) for T_a,

$$T_a = \frac{AT_L}{1 - A} + \frac{T_0}{G_m} - T_m . \tag{5}$$

Since the terms on the right of (5) are determined by independent measurement, the noise temperature due to the back lobes is obtained from

$$T_b = T_a - T_s - T_l \tag{6}$$

provided T_s and T_l are known.

The sky temperature, T_s, for an atmosphere of given humidity is known from experience.* The transmission line contribution, T_l, is measured independently as discussed in Appendix A.

3.3 *Method of Gain and Radiation Pattern Measurement*

Gain measurements were made by comparing the power received by the antenna with that of a standard horn. A height run was made with this horn over the vertical extent of the main paraboloid for each gain measurement, the average of these data being taken as the reference value. Using the same equipment, azimuthal radiation patterns were obtained for the two principal polarizations.

IV. MEASUREMENTS ON THE SHALLOW PARABOLOID ($f/D = 0.375$)

4.1 *Noise Measurements Using Various Feeds*

The 16-foot diameter spun-aluminum shallow paraboloid ($f/D = 0.375$) was first fed in a conventional manner using a cylindrical waveguide horn supported at the focal point by fiber glass struts, the feed waveguide running out from the apex. The radiation pattern of this

* In assigning values to T_s, the absolute water vapor density at the ground is determined from humidity and temperature measurements at the receiving site. Based on the particular value of water vapor density obtained, theoretical sky temperatures which have been verified previously[7] are calculated.

feed tapers to about −10 db at the rim of the paraboloid; this, in addition to an inverse distance effect of 3 db, results in a net illumination taper of 13 db.

Using the method for measuring noise discussed in Section 3.2, the two measurements on the curve of Fig. 7 labeled A were obtained* for zenith angles (θ) of zero and 45°. In spite of the relatively strong taper, this feed produces a noise temperature of 26°K at both angles. By removing the fiber glass mounting struts and supporting the feed with fine guy ropes, the point labeled B was obtained, T_b = 13.5°K. Comparison of the zenith point on curve A with point B shows that the fiber glass struts contribute 12.5° of noise. Strut noise can be produced both by reflection of noise radiated from the ground into the antenna and by loss in the material comprising the strut; this point is elaborated upon later.

The second feeding arrangement measured on this paraboloid was a standard Cassegrain consisting of a precision hyperboloid (whose diameter could be changed from 30 to 24 inches by removal of an outer ring) fed by a horn of 3.5λ diameter located at the apex of the main dish. The transmission line from horn to maser was about six feet of oversized circular guide including a right-angle bend.

With the hyperboloid mounted on fiber glass struts, noise measurements (at the zenith) produce T_b = 24.5°, as shown by point C in Fig. 7. The fiber glass struts were then covered with aluminum foil, essentially converting them to metal struts of the same geometry, and another measurement made, as indicated by the zenith value on curve D. At zenith the noise is now T_b = 11°K. Comparing this value with the 24.5° obtained using fiber glass struts, one sees that a decrease in noise of 13.5° has been effected. This result shows that most of the noise (at least for zenith orientation of the beam) is produced by loss in the dielectric; this conclusion seems to be valid because the decrease of 13.5° compares very favorably with the 12.5° decrease in T_b obtained when the fiber glass struts were removed during the test using the waveguide feed. Measurements were also made versus zenith angle, as shown by the remainder of curve D in Fig. 7. As the horizon is approached, T_b reaches values of the order 50°K. This noise is produced by spill-over beyond the rim of the hyperboloid and by reflection of noise from the earth by the sizable struts.

The last feeding arrangement to be discussed is the near-field Cassegrainian configuration. Fig. 5 shows a front view; mounted near the

* It may be well to mention here again that T_b in Fig. 7 is the intrinsic antenna noise; sky and waveguide noise, etc. are not included.

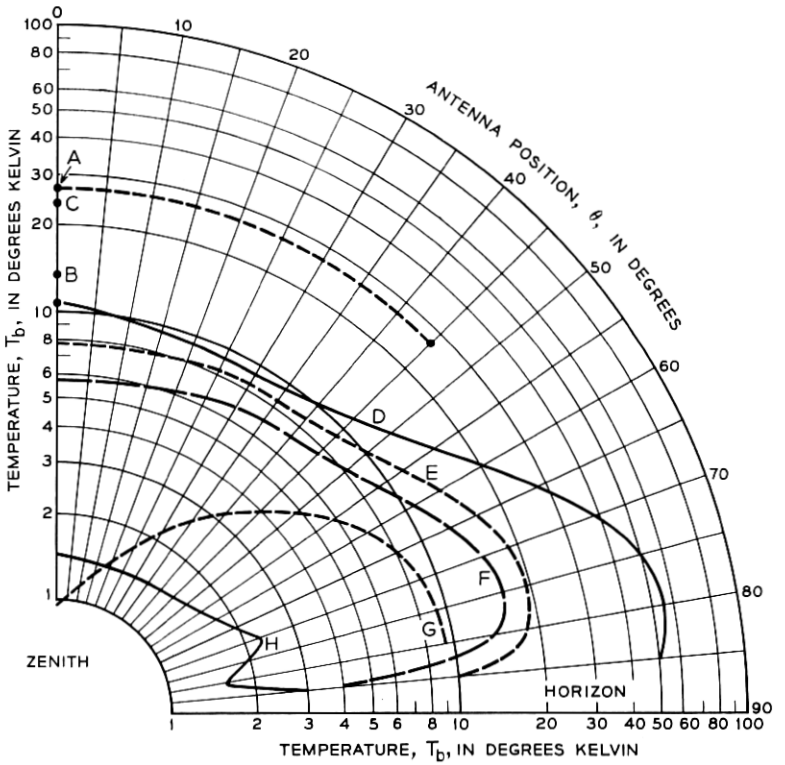

A. HORN-FED PARABOLOID, FIBERGLASS STRUTS
B. HORN-FED PARABOLOID, NO STRUTS
C. STANDARD CASSEGRAIN, FIBERGLASS STRUTS
D. STANDARD CASSEGRAIN, METAL STRUTS
E. NEAR-FIELD CASSEGRAIN, SUBREFLECTOR f=12″
F. AS E, NO STRUTS, MYLAR SUPPORT
G. CONICAL HORN REFLECTOR, 27″APERTURE
H. HORN REFLECTOR, 5′APERTURE (CRAWFORD HILL SITE, REFERENCE 7)

Fig. 7 — The 6-gc noise performance of 16-foot paraboloid (f/D = 0.375).

focal plane is one of the several paraboloids used as primary reflectors. The mounting struts are of interest; they are metallic, light-weight, small, and extend to the rim of the secondary reflector, the latter being done so that the struts do not intercept direct radiation from the sub-reflector.

Noise data obtained for this feed using a primary reflector of 12-inch focal length are shown in Fig. 7 as curve E. T_b at the zenith for this

arrangement is less than 8°K. Equally important, however, T_b is less than 20°K in the region of $\theta = 80°$, which is approximately the acquisition angle in a satellite communication system. At this angle the sky noise[7] is relatively high compared to the zenith value and it is desirable to have T_b as low as possible.

By using a subreflector of longer focal length (14.5 inches), much less spill-over of the secondary reflector occurs and a zenith temperature of 4°K was achieved. For all elevation angles with this subreflector, T_b was of the order of one-half that obtained with the subreflector of 12-inch focal length; of course, the secondary area illuminated is rather small and the gain is reduced by about 1.5 db; thus use of such subreflectors is of questionable value. A discussion of the signal-to-noise ratio in antennas is given in Appendix C.

To pursue the strut-noise effect further, a pressurized Mylar sheath support (similar to that shown in Fig. 9) with a wall thickness of 1.5 mils and inflated with nitrogen to a pressure of 0.15 psi was devised; it provides a remarkably rigid support. Nichrome guy wires from the subreflector to the rim of the secondary reflector are used for centering. Noise data for this arrangement (curve F in Fig. 7) show that there is an improvement of about 2°K (compared with curve E) for all elevation angles.

Curves G and H are included in Fig. 7 to serve as reference data. Curve G was obtained using the 27-inch horn-reflector feed (itself a low-noise antenna of respectable size with a far-field beamwidth of about 5°) mounted on the 16-foot paraboloid, struts and subreflector being removed. The arrangement amounts to a well shielded horn reflector with a large baffle (the secondary reflector); as indicated in curve G, T_b is less than 1°K at zenith. The rather rapid increase to $T_b = 9°K$ at $\theta = 80°$ is attributed in part to the limited horizon* mentioned in Section 3.1. Curve H was obtained using a five-foot horn reflector at the Crawford Hill site, which has a clear horizon.[7]

4.2 *Radiation Pattern, Gain, and Impedance*

The idealized near field of the conical horn feed was shown in Fig. 1 as a plane wave perfectly collimated in the direction of the primary reflector. In reality this is not the case; as discussed in connection with Fig. 4, the phase varies as much as $\pm 10°$ in places and is unsymmetrical with respect to the Z axis, as is the amplitude. From an academic point

* The decrease in noise very near the horizon shown by the curves in Figs. 7 and 10 is also attributed to the environment; this effect was not observed using the Crawford Hill site (Refs. 5 and 7).

of view, a plane-wave source with a symmetrical aperture field (such as a horn-lens antenna) would be preferable as the feed, since the unsymmetrical phase produced by the horn reflector produces unsymmetrical radiation patterns in the near field. Evaluation of the field distribution in the aperture of the main dish is also a near-field diffraction problem. Preliminary calculations, using idealized fields, indicate that this distribution is toroidal; the secondary patterns produced therefore have relatively high immediate side lobes, similar to those of a heavily blocked aperture.

Fig. 8(a) shows the measured pattern for longitudinal (horizontal) polarization, using the subreflector of 12-inch focal length. Note that the side lobes are unsymmetrical and that the highest one is only some 13.5 db down from the main lobe. In Fig. 8(b), for transverse (vertical) polarization, the immediate side lobes are more than 20 db down. In both cases the half-power beamwidth is about 0.7°. For comparison, a calculated curve for constant amplitude distribution and 2 per cent aperture blocking is also shown in Fig. 8. The gain is 48.0 db for transverse and 47.4 db for longitudinal polarization. The calculated full area gain of the 16-foot dish is 50.1 db at 6.3 kmc; thus the average effective area is 2.4 db down or, in other words, the efficiency is 57.5 per cent.

The SWR for the above configuration is 1.17, equivalent to a return loss of 22 db. A slight improvement in impedance is obtained by remov-

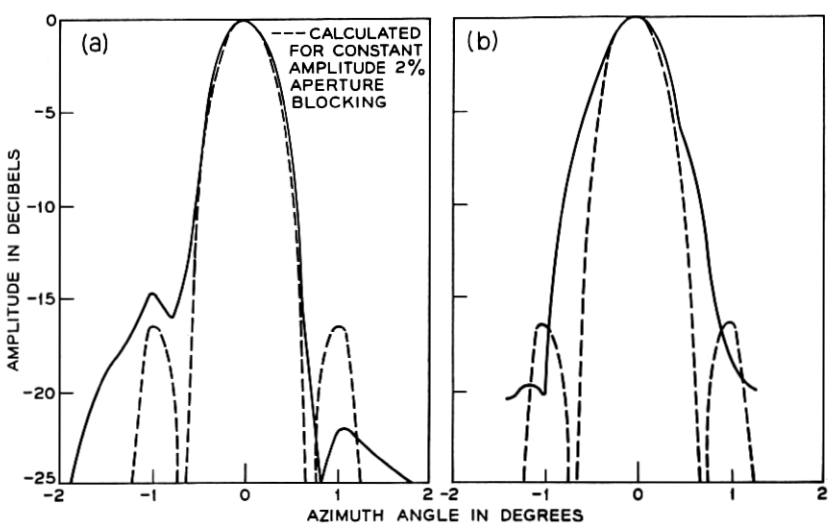

Fig. 8 — Radiation patterns of shallow paraboloid.

ing a circular area from the subreflector and illuminating the *concave* surface of the subreflector in the proper phase. This supplementary feeding arrangement (shown clearly in Fig. 5) resulted in a VSWR of 1.15 or a return loss of 23 db.

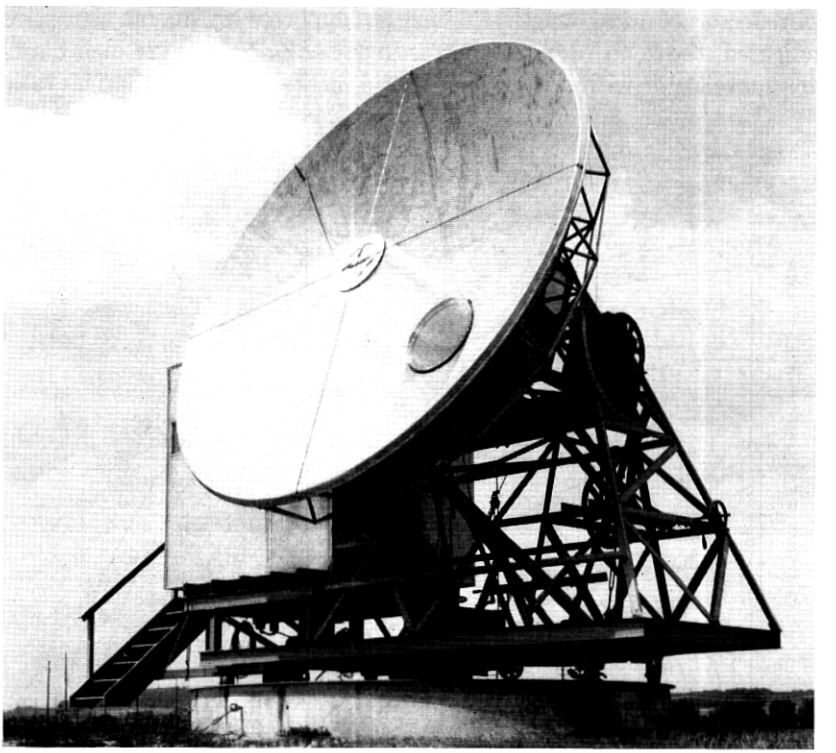

Fig. 9 — 16-foot paraboloid (f/D = 0.25) with near-field Cassegrainian feed. Note Mylar support for subreflector.

V. MEASUREMENTS ON THE DEEP PARABOLOID (f/D = 0.25)

5.1 *Noise Measurements Using Various Feeds*

Performance was next examined using a deep paraboloid (f/D = 0.25) as secondary reflector; Fig. 9 shows a front view. This paraboloid (diameter 16 feet) was machined from urethane foam, a reflective surface of zinc being applied after machining.* Near the focal plane is one of the

* Precision in reflecting surfaces is an important factor in determining the wide angle lobes[15] and therefore the noise performance of antennas.

paraboloids used as a primary reflector, in this case supported by a Mylar sheath. An alternative support used four half-inch struts extending perpendicularly from the mounting ring surrounding the feed aperture to the subreflector.

Curve A of Fig. 10 shows data obtained using a 30-inch diameter subreflector of focal length 7.5 inches supported by metal struts; as indicated, the zenith temperature is about 4°K. Next, a 24-inch diameter subreflector with a focal length of 6 inches was used, the f/D ratio

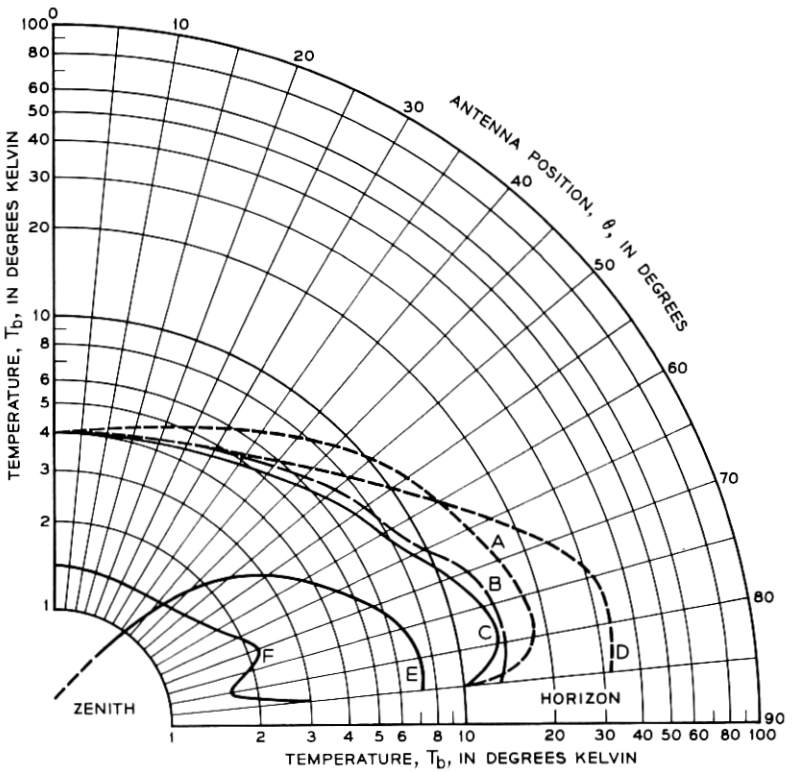

A. NEAR-FIELD CASSEGRAIN, SUBREFLECTOR f/D = 0.25, D = 30″
B. NEAR-FIELD CASSEGRAIN, SUBREFLECTOR f/D = 0.25, D = 24″
C. SAME AS B, NO STRUTS, MYLAR SUPPORT
D. STANDARD CASSEGRAIN
E. CONICAL HORN REFLECTOR, 27″APERTURE
F. HORN REFLECTOR, 5′ APERTURE
(CRAWFORD HILL SITE, REFERENCE 7)

Fig. 10 — The 6-gc noise performance of 16-foot paraboloid (f/D = 0.25).

being the same as in case A. As indicated by curve B, this feed arrangement displays very good characteristics, also achieving a zenith temperature of 4°K. Equally important, T_b remains less than 10°K until a zenith angle of sixty-five degrees is reached. In the region of $\theta = 80°$, T_b is less than 15°K.

Even though the struts supporting the subreflector were of small size, it was of interest to see what the change in T_b would be if the struts were removed. Fig. 9 shows the nitrogen-filled Mylar sheath (previously discussed in Section 4.2) supporting the 24-inch diameter subreflector, and curve C in Fig. 10 shows the data obtained. There is no appreciable change in the zenith noise temperatures; however, there is improvement for angles approaching the horizon, indicating that the small struts were to some extent scattering the earth's radiation into the antenna.

A standard Cassegrain feed consisting of a precision 30-inch diameter hyperboloid machined from styrofoam and suitably surfaced with zinc and a 3.5λ diameter horn located at the apex of the secondary reflector was tested for comparison with the near-field feed; the noise measurements are shown as curve D in Fig. 10. At zenith, the noise temperature is 4°K, but spill-over effects quickly become apparent when the zenith angle exceeds sixty degrees. At $\theta = 80°$, T_b has increased to about 30°K; this is attributed mainly to spill-over beyond the rim of the subreflector.

Reference curves E and F are included in Fig. 10; similar data were discussed in connection with Fig. 7.

5.2 *Radiation Pattern, Gain and Impedance*

Fig. 11 shows the azimuth patterns for the deep dish using the 24-inch diameter paraboloid as primary reflector. In Fig. 11(a) (longitudinal polarization) the immediate side lobes are unsymmetrical and the highest one is about 13.0 db down. Figure 11(b) is the secondary pattern for transverse polarization in the feed. In both cases, the 3-db beamwidth is about 0.7°.

During the measurements, the well known problem of properly illuminating a deep paraboloid became apparent; however, it was readily determined that deep reflectors may be illuminated more easily by Cassegrainian techniques than by focal point feeds. For example, using the near-field feed, the illumination at the rim of a 30-inch subreflector is down about 13 db; including a 6 db inverse distance attenuation, the resulting taper across the secondary reflector is approximately 20 db. The measured gain was 4 db down from full area. By reducing the diameter of the subreflector, the taper is also reduced, thereby in-

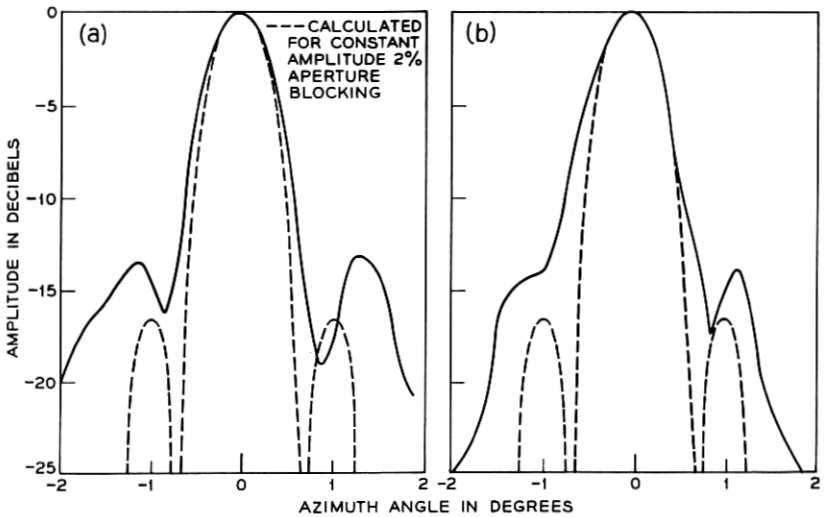

Fig. 11 — Radiation patterns of deep paraboloid.

creasing the gain (in this process, noise performance is often sacrificed for gain). A 24-inch subreflector was found to be a suitable compromise, measured gain for both polarizations being 47.3 db (2.8 db down from area). Somewhat surprisingly, as indicated by curve B of Fig. 10, there is no significant deterioration in noise performance.

Average SWR measurement for the configuration last mentioned is 1.11, which is equivalent to a return loss of 25 db, an improvement of 3 db over that of the shallow dish.

The gain of the standard Cassegrainian configuration was 47.4 db and 47.7 db for the vertical and horizontal polarizations, the average value being 0.24 db higher than that of the near-field device.

VI. DISCUSSION

The measurements discussed here have been directed toward evaluation of the noise performance of several types of feeds for full paraboloidal reflectors. In particular, it is found that the near-field Cassegrainian feed, a device whose design is based on simple geometrical optics, performs exceptionally well, its low-noise characteristics being as good or better than those of the standard Cassegrainian feed over all angles of elevation. This result holds true for both shallow and deep secondary

reflectors. The efficiency of the near-field Cassegrain is about 55 per cent, similar to that obtained using more conventional feeds; the radiation patterns are unsymmetrical due to lack of symmetry in the phase of the primary field.

Deterioration in noise performance due to the struts (or spars) used for supporting feed structures has been examined. Dielectric struts, such as those of fiber glass, have been found to introduce noise because of loss in the material. A pressurized membrane has been tested as a support for subreflectors; it appears satisfactory mechanically and minimizes degradation in electrical performance.

VII. ACKNOWLEDGMENTS

We are indebted to R. Kompfner for suggestion of the compression cylinder as a subreflector support, to A. B. Crawford for his interest in these studies, to H. W. Anderson for assistance in mechanical design, to L. E. Hunt, Tingye Li, and Mrs. C. L. Beattie for help in measurement and calculation of the near field of the conical horn-reflector, and to J. S. Cook for constructive comment. H. A. Gorenflo provided valuable assistance throughout the construction and measurement phases of these experiments.

APPENDIX A

Transmission Line Measurements

A.1 *Noise Measurements (Short Circuit)*

The noise that exists in a transmission line is caused by resistive losses in the line itself and by noise generators which may be at either or both ends of the line. Consider the infinite transmission line of Fig. 12(a), which for the moment is assumed to have a noise-free measuring device at terminal A. Let the thermodynamic temperature of the line be T_l, and α the power absorption coefficient. Since the line is of infinite length, the noise temperature measured at A is simply $T_a = T_l$. Divide the line into segments 1 and 2 at point l. The contribution to the noise at A by segment 2 is $T_l e^{-\alpha l}$ (since the line is infinite); therefore that contributed by segment 1 is $T_l(1 - e^{-\alpha l})$. A series expansion gives

$$T_l(1 - 1 + \alpha l - (\alpha^2 l^2/2) + \cdots)$$

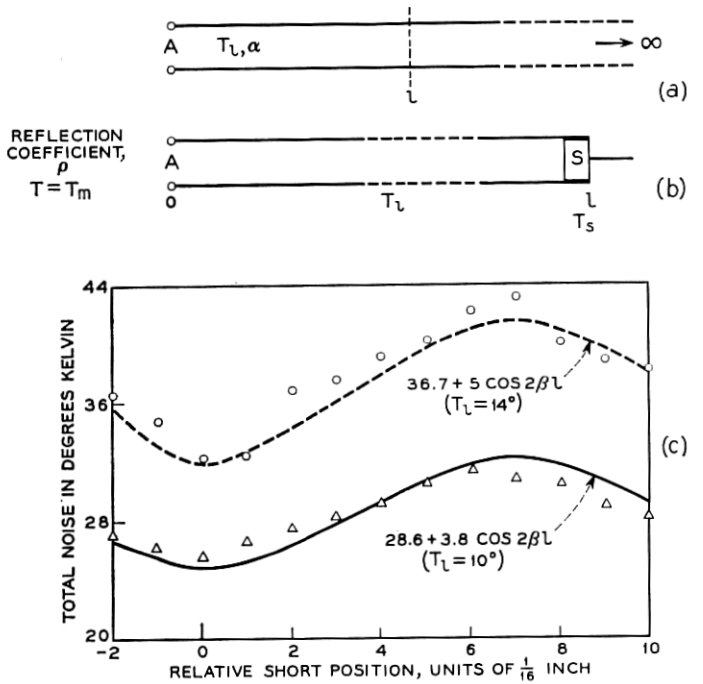

Fig. 12 — Noise measurements on shorted transmission line.

which for small α is approximately $T_l \alpha l$. Naturally, if the total loss, αl, is known, the noise produced is obtained immediately.*

Fig. 12(b) shows a movable shorting piston, S, near the terminals A of the amplifier to be used for the noise measurements. The amplifier is not perfectly noise free, nor is it perfectly matched; therefore movement of the piston produces a cyclical variation in the noise at A.

Let the effective temperature of the maser amplifier at terminals A in Fig. 12(b) be designated T_m ; this represents the intrinsic noise, which amounts to about 3°K. T_l represents the effective temperature of the transmission line and T_s that of the shorting piston, S. The voltage reflection coefficient at A (the input mismatch of the maser) is ρ. The

* This assumes that the thermodynamic temperature of the line is constant; if not, the effective noise temperature is given by

$$T = \int_0^l T(x)\alpha(x) \exp\left(-\int_0^x \alpha(x)\, dx\right) dx$$

where $T(x)$ is the temperature distribution along the line.

sources that give rise to noise T, traveling to the left (i.e., into the amplifier) at A are:

T_{m_1} — intrinsic amplifier noise;
T_{m_2} — amplifier noise traveling to the right, and reflected at S (uncorrelated with T_{m_1});
T_{l_1} — line noise initially traveling to right and reflected by S, also that reflected by ρ at A and again by S;
T_{l_2} — line noise initially traveling to left, also that reflected by ρ and by S (uncorrelated with T_{l_1});
T_S — shorting piston noise, traveling to left, also that reflected by ρ and by S.

Thus, to first order the noise entering the amplifier at A is

$$T = T_{m_1} + T_{m_2} + T_{l_1} + T_{l_2} + T_S .$$

If the attenuating effects of line loss are neglected (since they are only of the order 0.1 db), the above sum to first order becomes

$$T = T_{m_1} + (T_{m_2} + 2T_l + T_S)(1 + \rho^2) + 2(T_{m_2} + 2T_l + T_S)\rho \cos 2\beta l \tag{7}$$

where

$$2T_l = T_{l_1} + T_{l_2}$$

β being the propagation constant of the line.

Measured data (noise versus short position) shown as crosses in Fig. 12(c) were taken using a short circuit in round waveguide. Also shown (as a solid curve) are data calculated using the following constants in (7): $T_{m_1} = 3°$, $T_{m_2} = 3°$, $T_l = 10°$, $T_S = 2.5°$ (short circuit with a standing wave ratio of 250) and $\rho = 0.075$ (22-db return loss), the last two being measured values; these result in

$$T = 28.6 + 3.8 \cos 2\beta l. \tag{8}$$

Now let an additional length of transmission line be added to l such that the total length is l_1, and let the short S be moved to the end of this line. The data, shown as dots in Fig. 12(c), were obtained when approximately 6 feet of 2.8-inch diameter line* were added. The dashed curve is a plot of (7) with the following constants:

$$T_{m_1} = T_{m_2} = 3°, \qquad T_{l_1} = 14°, \qquad T_S = 2.5°, \qquad \rho = 0.075,$$

$$T_1 = 36.7 + 5.0 \cos 2\beta l. \tag{9}$$

* The line actually comprised 45 inches of straight guide and a right-angle bend of 15-inch radius used in the standard Cassegrain feed.

If (8) is subtracted from (9), one has

$$2(T_{l_1} - T_l)(1 + \rho^2) + 4(T_{l_1} - T_l)\rho \cos 2\beta l = 7.9 + 1.2 \cos 2\beta l. \tag{10}$$

From the first terms of both sides of (10), one obtains $2(T_{l_1} - T_l) = 7.9$, or an increased noise temperature $T_{l_1} - T_l = 3.95°$ due to the additional length of line. From the second terms one obtains $4(T_{l_1} - T_l)\rho = 1.2$ or $T_{l_1} - T_l = 4°$. The accuracy of the latter value is very dependent upon an accurate value for ρ (measured as 0.075), whereas the first value, 3.95° (which is really the difference between the average values of the plots in Fig. 12(c), is good to order $1 + \rho^2$. The value 3.95°K is equivalent to a loss of 0.052 db in the additional length of line.

A.2 *SWR Measurements (Short Circuit)*

Using the same shorting piston and transmission line as above but adding an additional 60-inch length of waveguide (diameter 2.8 inches), the measured VSWR was 85, which is equivalent to a loss of 0.0093 db/foot.

The loss per unit length derived from the noise measurement just discussed is 0.0092 db/foot, indicating close agreement between the two methods.

APPENDIX B

The Antenna Noise — T_b

Since typical antenna patterns have significant levels in the side and back lobes, it is necessary to consider the effects of noise due to thermal radiation from the environment into the antenna.* This effective noise temperature is designated by T_b.

Consider first the ideal radiation pattern shown in Fig. 13(a): it has a very narrow beam of width α, the gain G being constant over the angle α; it has no back lobes. The antenna is assumed to be lossless and to be mounted height h above the ground. Beamed at various angles θ with respect to zenith, this antenna sees the true brightness temperature, $T(\theta)$, due to various noise sources. For $0 < \theta < \pi/2$, $T(\theta) = T_s(\theta)$ is the sky temperature. For $\pi/2 < \theta < \pi$, the brightness temperature is due to both sky and earth, as shown in Fig. 13(b), since the sky noise from angle $\pi - \theta$ is reflected at point P according to the reflection

* This effect has been discussed recently in Ref. 16.

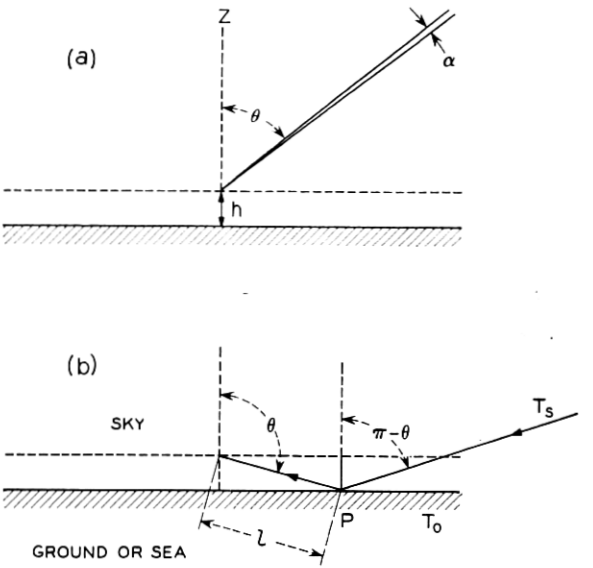

Fig. 13 — Ideal antenna and its environment.

coefficient of the earth, $r(\theta)$, at P, whereas the earth generates noise that enters the antenna directly dependent upon the coefficient $a(\theta)$, which represents absorption at P. Noise due to loss in the atmosphere along path length l also contributes to the brightness temperature. Since $r(\theta) + a(\theta) = 1$, the brightness temperature for $\pi/2 < \theta < \pi$ is

$$T(\theta) = r(\theta)T_s(\pi - \theta) + [1 - r(\theta)]T_0 + T_{s_l}(\theta - \pi/2) \quad (11)$$

where T_0, the temperature of the ground, is assumed to be 300°K.

The term $T_{s_l}(\theta - \pi/2)$ of (11) represents noise due to the path in the atmosphere between the antenna and the point P. Compared with other noise sources, it is found to be negligible, and therefore has been disregarded in what follows.

The reflection coefficient $r(\theta)$ is highly dependent upon the environment and to some extent on polarization; it usually varies with time, being a function of the ground conditions over vegetated areas and the wave conditions over water. Using representative data at 10 cm wavelength for the reflection coefficient,[17] the sky temperature, and (11), one can estimate the brightness temperature distribution for all angles θ, as shown in Fig. 14. Curve B is for smooth sea water and curve A for a perfectly reflecting mirror (which images the sky noise), whereas the

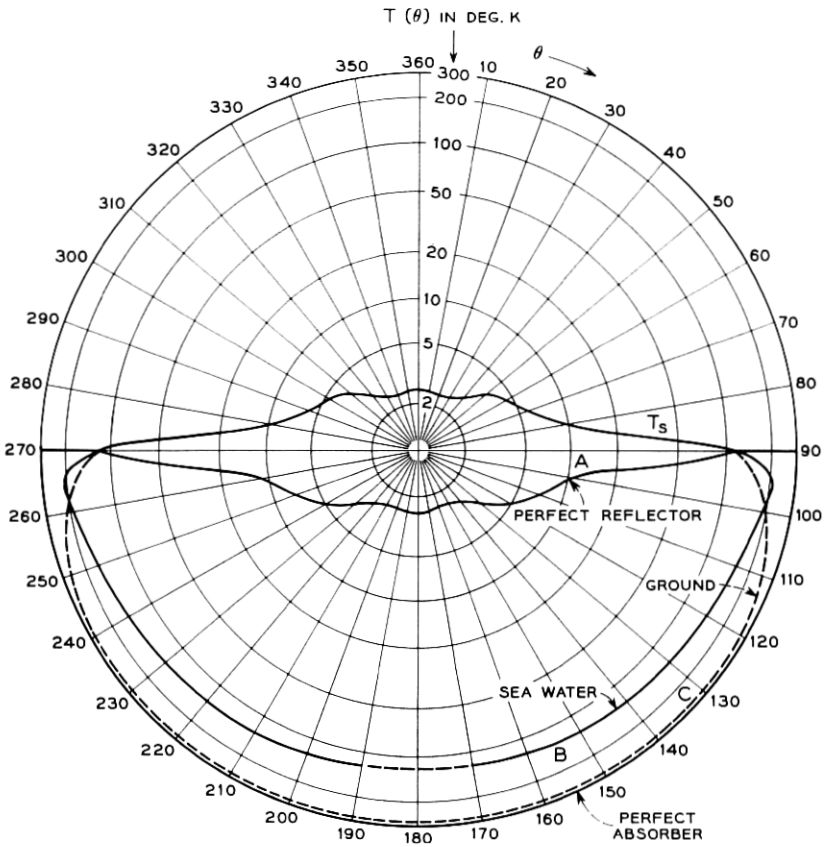

Fig. 14 — Brightness temperature distributions for middle cm-wave band.

poorly reflecting ground environment, curve C, approximates a perfect absorber.

An actual antenna has a finite radiation pattern $G(\theta)$; assuming it to be symmetrical about the main axis of the antenna beam, the equation relating antenna temperature to radiation pattern and brightness temperature is

$$T_s + T_b = \frac{1}{2}\int_0^{\pi} G(\theta)T(\theta)\sin\theta\, d\theta \tag{12}$$

for the antenna beamed vertically. If the antenna is beamed at angle θ' with respect to the zenith, (12) becomes

$$T_s(\theta') + T_b(\theta') = \frac{1}{2}\int_0^{\pi} G(\theta - \theta')T(\theta)\sin\theta\, d\theta. \tag{13}$$

As a simple application of (12), consider an isotropic antenna surrounded by a noise-free sky and a perfectly absorbing earth. In this case $G(\theta) = 1$ and $T(\theta) = T_0$ for $\pi/2 < \theta < \pi$; thus

$$T_s + T_b = \frac{1}{2}\int_{\pi/2}^{\pi} T_0 \sin\theta \, d\theta = \frac{T_0}{2} = 150°\text{K}.$$

An idealized radiation pattern for a microwave antenna is shown in Fig. 15, where

$$G(\theta) = G_0, \qquad 0 < \theta < \alpha/2$$

and

$$G(\theta) = G_b, \qquad \alpha/2 < \theta < \pi,$$

G_b being the average gain in the side and back lobes. Again assuming a noise-free sky and perfectly absorbing earth,

$$T_{b_2} = \frac{1}{2}\int_{\pi/2}^{\pi} G_b T_0 \sin\theta \, d\theta = \frac{T_0 G_b}{2} = 150 G_b °\text{K}.$$

Thus, for example, if $G_b = 0.1$ (10 db below isotropic), $T_{b_2} = 15°\text{K}$.

Using the idealized antenna pattern of Fig. 15 and the data of Fig. 14, let us now integrate numerically according to (12). The noise contribution from the main beam (the so-called sky noise) is

$$T_s = \frac{1}{2}\int_0^{\alpha/2} G_0 \, T_s(\theta) \sin\theta \, d\theta \approx 2.5°$$

which is readily taken from Fig. 14.

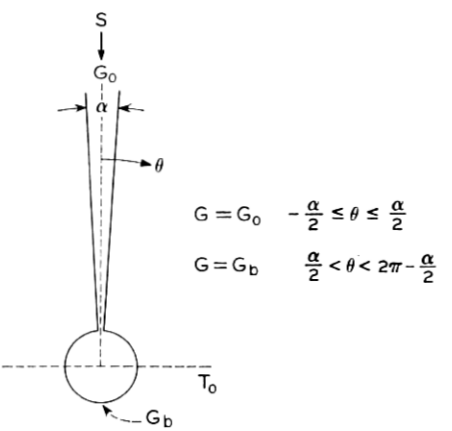

Fig. 15 — Idealized antenna pattern.

Using $G_b = 0.1$, the contribution due to sky noise in the far side lobes ($\alpha/2 < \theta < \pi/2$) is

$$T_{b_1} = \frac{G_b}{2} \int_{\alpha/2}^{\pi/2} T_s(\theta) \sin \theta \, d\theta = 0.7°.$$

From the region $\pi/2 < \theta < \pi$ (ground, etc.), the contribution is

$$T_{b_2} = \frac{G_b}{2} \int_{\pi/2}^{\pi} T(\theta) \sin \theta \, d\theta$$

which amounts to 0.7° for the antenna above a perfect reflector, 7.6° above sea water and 15° above a perfectly absorbing earth.

Thus for an antenna with far side and back lobes 10 db below an isotropic radiator, the total antenna noise due to atmosphere and environment for zenith orientation of the beam is

$$T_a = T_s + T_{b_1} + T_{b_2}$$

which amount to 3.9° (perfect reflector)
10.8° (calm sea water)
18.2° (ground with vegetation which approximates a perfect absorber).

$T_b = T_{b_1} + T_{b_2}$ for the above conditions is
1.4° (perfect reflector)
8.3° (calm sea water)
15.7° (ground with vegetation)
obtained simply by subtracting the sky noise (2.5°K) from the previous numbers.

APPENDIX C

The Signal-To-Noise Ratio and Quality Factor of an Antenna

For the idealized antenna pattern of Fig. 15, the received power at the terminals of the antenna oriented toward a white noise signal source is

$$P_S = SAB = SG_0(\lambda^2/4\pi)B$$

where S is the incident signal flux, B the bandwidth, and A the effective area of the antenna. The total noise in the antenna is $P_N = kT_aB$, k being Boltzmann's constant and $T_a = T_s + T_b + T_l$. The contribution T_s is the sky noise in the main beam; it is essentially independent of the gain G_0 for high-gain antennas. T_b and T_l are the effective noise temperatures due to back lobes and line losses. The signal-to-noise ratio

for the antenna is therefore

$$\frac{P_S}{P_N} = \frac{S\lambda^2}{4\pi k}\frac{G_0}{T_a} = \frac{S\lambda^2}{4\pi k}\frac{G_0}{(T_s + T_b + T_l)}. \tag{14}$$

This assumes that the noise figure of the receiving amplifier is negligible. Of course, the receiver noise and the antenna impedance must both be considered in calculating the system noise.

Of the terms contributing to T_a in (14), T_s is unavoidable and only T_b and T_l can be attributed to deficiencies in the antenna. We can define a quality factor for the antenna in the following way: set T_s equal to zero and multiply numerator and denominator of (14) by T_0; then

$$\frac{P_S}{P_N} = \frac{S\lambda^2}{4\pi k T_0}\frac{G_0 T_0}{(T_b + T_l)} = \frac{S\lambda^2}{4\pi k T_0} Q \tag{15}$$

where $Q = G_0 T_0/(T_b + T_l)$ is the quality factor. Examples of typical values of Q are:

(1) An isotropic antenna completely surrounded by a perfect absorber at $T_0 = 300°$ ($T_l = 0$, no line losses), $Q = 1$.

(2) An isotropic antenna surrounded by a perfectly absorbing earth and noise-free sky, (no line losses), $Q = 2$.

(3) The antenna above ground as discussed in Appendix B with far side and back lobes 10 db below an isotropic radiator, (where $T_b \approx 15°$), $Q = 20G_0$.

(4) The near-field Cassegrain as discussed in Section V

$$(G_0 = 5.4 \times 10^4, \qquad T_l + T_b = 4° + 4° = 8°), \qquad Q = 2 \times 10^6.$$

(5) A horn-reflector antenna with the same aperture area and transmission line loss as in (4) above

$$(G_0 = 7 \times 10^4, \qquad T_l + T_b = 4° + 1° = 5°), \qquad Q = 4.2 \times 10^6.$$

Similarly, one can define a quality factor for the total receiving system as

$$Q_T = \frac{G_0 T_0}{T_R + T_a}$$

where T_R represents all noise associated with the receiver proper, and T_a, all noise associated with the antenna.

REFERENCES

1. Crawford, A. B., Hogg, D. C., and Hunt, L. E., A Horn-Reflector Antenna for Space Communication, B.S.T.J., **40**, July, 1961, p. 1095.

2. Hines, J. N., Li, Tingye, and Turrin, R. H., The Electrical Characteristics of the Conical Horn-Reflector Antenna, B.S.T.J., **42,** July, 1963, p. 1187.
3. Giordmaine, J. A., Alsop, L. E., Mayer, C. H., and Townes, C. H., A Maser Amplifier for Radio Astronomy at X-Band, Proc. IRE, **47,** No. 6, 1959, p. 1064.
4. Cook, J. J., Gross, L. G., Bair, M. E., and Terhume, R. W., A Low-Noise X-Band Radiometer Using Maser, Proc. IRE, **49,** No. 4, 1961, p. 768.
5. DeGrasse, R. W., Hogg, D. C., Ohm, E. A., and Scovil, H. E. D., Ultra-Low-Noise Receiving System for Satellite or Space Communications, Proc. Nat. Electr. Conf., **15,** 1959, p. 370.
6. Ohm, E. A., Receiving System — Project Echo, B.S.T.J., **40,** July, 1961, p. 1065.
7. Hogg, D. C., and Semplak, R. A., The Effect of Rain and Water Vapor on Sky Noise at Centimeter Wavelengths, B.S.T.J., **40,** Sept., 1961, p. 1331.
8. Hannan, P. W., Microwave Antennas Derived from the Cassegrain Telescope, IRE Trans. on Antennas and Propagation, **AP-9,** March, 1961, p. 140.
9. Potter, P. D., Aperture Efficiency of Large Paraboloidal Antennas as a Function of their Feed System Radiation Characteristics, IEEE Trans. on Antennas and Propagation, **AP-11,** May, 1963.
10. Profera, C. E., and Sciambi, A. F., A High Efficiency Low-Noise Antenna Feed System, PTGAP International Symposium, Boulder, Colorado, July, 1963.
11. Morgan, S. P., Some Examples of Generalized Cassegrainian and Gregorian Antennas, to be published in Nov., 1964, IEEE Trans. on Antennas and Propagation.
12. Cook, J. S., and Lowell, R., The Autotrack System, B.S.T.J., **42,** July, 1963, p. 1283.
13. Potter, P. D., Unique Feed System Improved Space Antennas, Electronics, **25,** June 22, 1962, p. 36.
14. Schelkunoff, S. A., and Friis, H. T., *Antennas Theory and Practice*, J. Wiley & Sons, 1952, Ch. 18.
15. Dragone, C., and Hogg, D. C., Wide-Angle Radiation Due to Rough Reflectors, B.S.T.J., **42,** Sept., 1963, p. 2285.
16. Croom, D. L., Naturally Occurring Thermal Radiation in the Range 1–10 Gcs, Proc. IEE, **3,** No. 5, May, 1964, p. 967.
17. Kerr, D. E., *Propagation of Short Waves*, McGraw-Hill Book Co., 1951, ch. 5.